

Shock Excitation of Emission Lines in GPS, CSS, and CSO Sources

Geoffrey V. Bicknell,¹ Michael A. Dopita,² and Christopher P. O’Dea³

¹*Astrophysical Theory Centre, Australian National University, Canberra, ACT 0200, Australia*

²*Mt. Stromlo and Siding Spring Observatories, Weston PO, ACT 2611, Australia*

³*Space Telescope Science Institute, 3700 San Martin Drive, Baltimore, MD 21218, USA*

1. Introduction

The classes of radio-loud AGN known as Gigahertz-peak spectrum (GPS), compact steep spectrum (CSS), and compact symmetric objects (CSO) represent an important sub-class of AGN, constituting, for example, 24% of the Baker, Hunstead, & Brinkmann (1995) sample. Table 1 summarizes some of their key properties.

Table 1. Properties of GPS, CSS, and CSO Sources

Source	Characteristics	General Properties
GPS	Peak in radio spectrum at GHz frequencies < Size > ≈ 350 pc < Pressure > $\approx 10^{-6}$ dyn cm ⁻²	< $F_{5\text{GHz}}$ > $\approx 10^{27.5}$ W Hz ⁻¹ RM ≈ 0 –1000 rad m ⁻²
CSS	Steep spectrum at GHz frequencies Spectral peak at ~ 100 MHz < Size > ≈ 10 kpc < Pressure > $\approx 10^{-8}$ dyn cm ⁻²	Strong forbidden line spectrum Forbidden-line widths ~ 500 –1000 km s ⁻¹
CSO	Compact, symmetric FR II-like morphology	

It is now clear (e.g., Stanghellini et al. 1996) that GPS and CSS sources differ only in the location of the peak frequency. Moreover, every CSO is a GPS source, and while the reverse is not strictly true, there is certainly a large overlap between GPS sources and CSOs and we assume that the interaction of the respective jets with the ISM in these classes is similar. For some time, it has been debated whether such sources are young or confined. Begelman (1996) proposed an elegant solution to this problem by constructing a model involving the interaction of young radio lobes with a dense power-law atmosphere. In Begelman’s view, the sources are relatively young ($\sim 10^6$ yrs) compared to FR II radio

galaxies, and his model provides a satisfactory explanation for the luminosity–size relation. We have developed this model for the purpose of explaining the correlation between emission-line luminosity and radio power (Gelderman & Whittle 1996) and peak turnover frequency and size (Stanghellini et al. 1996), thereby unifying the radio and optical properties of these objects.

2. Begelman’s Dynamical Model for Compact Symmetric Objects

Begelman’s (1996) model for ‘baby Cygnus As’ (modified to allow for adiabatic losses in the expanding cocoon) provides the basis for our modeling of the emission-line luminosity and peak-frequency–size relation. The averaged pressure at the head of the lobe is assumed to be a constant factor ζ times the average pressure in the rest of the lobe. Taking the ambient density, $\rho_a = \rho_0(x/x_0)^{-\delta}$, where ρ_0 and x_0 are fiducial values and the jet energy flux to be F_E , this model implies for the distance $x_h(t)$ of the hotspot from the core and for the average cocoon pressure $P_c(t)$

$$x_h = x_0 \xi^{1/(5-\delta)} \quad \text{and} \quad P_c = P_0 \xi^{(2-\delta)/(5-\delta)} \quad (1)$$

where

$$\xi = \frac{(5-\delta)^3 \zeta^2}{18\pi(8-\delta)} \left(\frac{F_E t^3}{\rho_0 x_0^5} \right) \quad \text{and} \quad P_0(t) = \frac{9}{\zeta(5-\delta)^2} \rho_0 \left(\frac{x_0}{t} \right)^2. \quad (2)$$

For the above-quoted average size and pressure for a GPS source, the jet energy flux and ambient density are $\sim 5 \times 10^{44} t_6^{-1}$ ergs s^{-1} and $100 t_6^2 \text{ cm}^{-3}$, respectively. Energy fluxes $\sim 10^{45}$ ergs s^{-1} are consistent with an age $\sim 5 \times 10^5$ yr and a ratio κ_5 of monochromatic power at 5 GHz to jet energy flux $\sim 10^{-11}$ – $10^{-10.5}$, a factor of a few higher than is normally assumed for FR II sources, but consistent with the luminosity–size evolution suggested by Begelman (1996).

The lateral expansion velocity of the cocoon as a function of distance is given by

$$V_c = V_0 \left(\frac{x_h}{x_0} \right)^{(\delta-2)/3} \quad (3)$$

where

$$V_0 \approx 1500 \left(\frac{6}{8-\delta} \right)^{1/3} \zeta^{1/6} \left[\frac{F_{E,45}}{n_{H,0}} \right]^{1/3} \text{ km s}^{-1}, \quad (4)$$

$10^{45} F_{E,45}$ ergs s^{-1} is the energy flux, and $n_{H,0}$ is the Hydrogen number density at $x_0 = 1$ kpc. For $F_{E,45}/n_{H,0} \approx 0.1$, the expansion velocity is of order the line widths observed by Gelderman & Whittle (1996).

3. Emission from Radiative Shocks

The bow shock advancing into the ISM is radiative for ambient densities greater than $\sim 10 \text{ cm}^{-3}$ and ages $\lesssim 10^{6-7}$ yrs. The total continuum plus emission-line luminosity L_T and [O III] luminosity $L([\text{O III}])$ from the shocked gas and

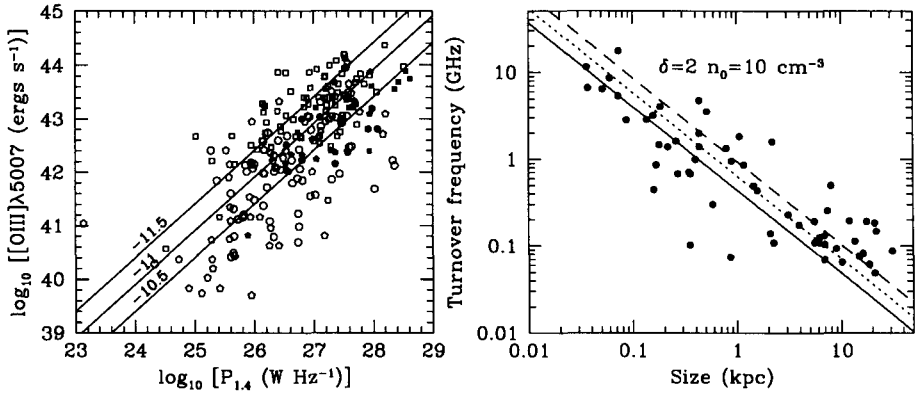


Figure 1. *Left:* Predicted [O III]-luminosity/radio-power relation for various values of $\log \kappa_{1.4}$ compared to the data for radio-loud AGN. Filled circles, filled squares, open circles and open squares represent CSS radio galaxies, CSS quasars, radio galaxies and radio-loud quasars, respectively, from Gelderman & Whittle (1996); filled hexagons and open hexagons are unresolved sources and radio galaxies from Tadhunter et al. (1993) and Morganti et al. (1993). *Right:* Turnover-frequency versus size relation compared to data from Stanghellini et al. (1996). Jet energy fluxes of 10^{45} , $10^{45.5}$ and 10^{46} ergs s^{-1} are represented by solid, dotted, and dashed lines, respectively.

photoionized precursor were calculated for a range of shock velocities using the MAPPINGS II emission-line code (Sutherland & Dopita 1993) and are given by (in units of ergs s^{-1})

$$L_T = 1.1 n_H V_3^3 A_{sh} \quad L([\text{O III}]) = 2.3 \times 10^{-2} n_H V_3^3 A_{sh}, \quad (5)$$

where A_{sh} cm^2 is the shock area. Equating L_T to the rate of work, $3/(8 - \delta)F_E$ done by the expanding lobe gives

$$L([\text{O III}]) = 8.2 \times 10^{42} \left(\frac{6}{8 - \delta} \right) \left(\frac{\kappa_{1.4}}{10^{-11}} \right)^{-1} \left(\frac{P_{1.4}}{10^{27} \text{ W Hz}^{-1}} \right) \text{ ergs } s^{-1} \quad (6)$$

where $\kappa_{1.4}$ is the ratio of 1.4 GHz radio power to jet energy flux. A comparison of this relation with the [O III] luminosities for radio galaxies and quasars from Gelderman & Whittle (1996) and radio galaxies from Tadhunter et al. (1993) and Morganti, Killeen, & Tadhunter (1993), is shown in the left-hand panel of Fig. 1. Established and candidate GPS, CSS, and CSO sources are indicated by filled symbols. Good agreement is obtained for $\kappa_{1.4} \approx 10^{-10.5}$. However, the [O III] fluxes of GPS sources are substantially reddened (Baker & Hunstead 1996) so that correspondingly smaller values of $\kappa_{1.4}$ may be relevant. Similar good agreement is obtained for the $H\alpha + [\text{N II}]$ data from Gelderman & Whittle (1996); see Bicknell, Dopita, & O'Dea (1996).

4. The Radio Spectra and the Peak-Frequency–Size Relation

Both the anticorrelation between peak frequency and size and the power-law slope at low frequency can be attributed to free-free absorption by the ionized shock and precursor regions. The free-free optical depth $\tau_\nu = a\nu_9^{-2.1}$, where $a = 1.1 \times 10^{-25} \int n_e^2 T_4^{-1.35} dl$. The contributions to a from uniform shock and precursor zones are $2.0 \times 10^{-3} V_3^{2.3} n_H$ and $1.0 \times 10^{-3} V_3^{1.5} n_H$ respectively, where $n_H \text{ cm}^{-3}$ is the pre-shock Hydrogen density and V_3 is the shock velocity in units of a thousand km s^{-1} . A uniform medium surrounding the lobes would give an $\exp[-a\nu^{-2.1}]$ cutoff to the spectrum. However, if we assume that a is distributed as a truncated power-law (probability density function $\propto a^p$ for constant p and $0 < a < a_0$), then the flux density is

$$F_\nu = A \left(\frac{\nu}{\nu_0} \right)^{2.1(p+1)-\alpha} \gamma(p+1, (\nu/\nu_0)^{-2.1}), \quad (7)$$

where A is a constant, α is the high-frequency spectral index, $\nu_0^{2.1} = a_0$, and $\gamma(p+1, x)$ is the incomplete gamma function. This spectrum peaks at $\nu \approx \nu_0$ and the low-frequency spectral index is $\alpha - 2.1(p+1)$. Evaluating p from the low-frequency spectral indices estimated by Stanghellini et al. (1996) gives $\langle p \rangle \approx -0.2$, close to a uniform distribution. It is most likely that *any* broad distribution of optical depths will lead to a spectrum of the required form. We take $\langle a \rangle$ to be the value predicted by the uniform one-dimensional MAPPINGS models so that the peak frequency is

$$\nu_p \approx 1.1 \left(\frac{p+2}{p+1} \right)^{0.48} \left[2.0 \times 10^{-3} V_3^{2.3} + 1.0 \times 10^{-3} V_3^{1.5} \right]^{0.48} n_0^{0.48} \left(\frac{x}{\text{kpc}} \right)^{-0.48\delta}. \quad (8)$$

This relationship is plotted (for $\delta = 2$) and favorably compared to the Stanghellini et al. (1996) data in the right-hand panel of Fig. 1. It can also be shown that the magnetionic medium surrounding the radio lobes produces substantial Faraday depolarization explaining another important characteristic of these sources. Thus, using quite straightforward physics, we have shown that the radio and optical properties of this class of AGN can be unified.

References

- Baker, J. C., & Hunstead, R. W. 1996, *ApJ*, 452, L95.
 Baker, J. C., Hunstead, R. W., & Brinkmann, W. 1995, *MNRAS*, 277, 553.
 Begelman, M. C. 1996, in *Cygnus A: Study of a Radio Galaxy*, ed. C. L. Carilli & D. A. Harris (Cambridge University Press: Cambridge).
 Bicknell, G. V., Dopita, M. A., & O’Dea, C. P., *ApJ*, submitted.
 Gelderman, R., & Whittle, M. 1996, *ApJ*, in press.
 Morganti, R., Killeen, N. E. B., & Tadhunter, C. N. 1993, *MNRAS*, 263, 1023.
 Stanghellini, C., O’Dea, C., Fanti, R., Baum S. A. 1996, in preparation.
 Sutherland, R. S., and Dopita, M. A. 1993, *ApJS*, 88, 253.
 Tadhunter, C. N., Morganti, R., di Serego Alighieri, S., Fosbury, R. A. E., & Danziger, I. J. 1993, *MNRAS*, 263, 999.